Australas Phys Eng Sci Med (2017) 40:277–287
DOI 10.1007/s13246-017-0530-x

SCIENTIFIC PAPER

Indices from lagged poincare plots of heart rate variability: an efficient nonlinear tool for emotion discrimination

Ateke Goshvarpour[1] · Ataollah Abbasi[1] · Atefeh Goshvarpour[1]

Received: 31 May 2016 / Accepted: 27 January 2017 / Published online: 16 February 2017

Abstract Interest in human emotion recognition, regarding physiological signals, has recently risen. In this study, an efficient emotion recognition system, based on geometrical analysis of autonomic nervous system signals, is presented. The electrocardiogram recordings of 47 college students were obtained during rest condition and affective visual stimuli. Pictures with four emotional contents, including happiness, peacefulness, sadness, and fear were selected. Then, ten lags of Poincare plot were constructed for heart rate variability (HRV) segments. For each lag, five geometrical indices were extracted. Next, these features were fed into an automatic classification system for the recognition of the four affective states and rest condition. The results showed that the Poincare plots have different shapes for different lags, as well as for different affective states. Considering higher lags, the greatest increment in SD_1 and decrements in SD_2 occurred during the happiness stimuli. In contrast, the minimum changes in the Poincare measures were perceived during the fear inducements. Therefore, the HRV geometrical shapes and dynamics were altered by the positive and negative values of valence-based emotion dimension. Using a probabilistic neural network, a maximum recognition rate of 97.45% was attained. Applying the proposed methodology based on lagged Poincare indices, a valuable tool for discriminating the emotional states was provided.

Keywords Affect · Classification · Lagged poincare plot · Heart rate

✉ Ataollah Abbasi
ata.abbasi@sut.ac.ir
http://ee.sut.ac.ir/Labs/CNLab/index.html

Ateke Goshvarpour
ak_goshvarpour@sut.ac.ir

Atefeh Goshvarpour
af_goshvarpour@sut.ac.ir

[1] Computational Neuroscience Laboratory, Department of Biomedical Engineering, Faculty of Electrical Engineering, Sahand University of Technology, New Sahand Town, PO. BOX 51335/1996, Tabriz, Iran

Introduction

Nowadays, the developments of computer-based human emotion recognition systems are attributed to the field of affective computing. The affective computing research area is young and rapidly developing. It tries to automatically recognize and appropriately respond to human emotional expressions, which make human–computer interactions more natural and pleasurable. To this effect, different emotion configurations (such as speech and facial expressions) with different emotion elicitation paradigms (such as video, music and images) and methodologies (such as linear and nonlinear signal and image processing techniques) have been examined [1–25].

Emotions can be measured in both discrete and dimensional perspectives. The former is based on the basic emotions (such as happiness, sadness, fear, and surprise) [1–3], whereas the latter is based on a 2D space (valence and arousal) to map the affective contents [4, 5]. Many emotion induction techniques have been used in the experiments, including visual paradigms (picture viewing [6] and film clips [7]), auditory stimulation (music [8, 9] and sounds [10]), real-life experiences [11], computer games [12], recall [13], and imagery [14]. All the above-mentioned techniques try to excite different emotions and they have some benefits and shortcomings.

To evaluate emotions, various methods have been also addressed in the literature such as physiological responses [15], gestures [16], facial expressions [17], vocal indications [18], and self-reports [19]. Among them, the physiological indices have received significant attention. Regarding the physiological signals, analysis of heart rate variability (HRV), as a quantifier of autonomic nervous system (ANS), has been extensively examined in the studies [20]. HRV is usually calculated from the RR intervals of electrocardiogram (ECG) signals. A typical ECG is the electrical activity of the heart. Morphologically, it consists of some peaks and valleys due to the action of different parts of the heart. The highest peak is called "R-peak". The heart rate can be determined by measuring the interval between R-peaks (RR interval). One method is to divide 60 by the RR intervals in seconds. In general, the variation in the time interval between R-peaks are considered as HRV.

Considering the cardiovascular systems, most of the human knowledge about the emotional behaviors and responses has been acquired by standard approaches. These indices were primarily established in the related literature and are still very common in signal processing. Standard features are mainly divided into the time- and frequency-based methods. Some examples of time-domain features are mean, standard deviation (SD), moments, SDRR (the standard deviation of the RR intervals), RMSSD (root mean square of the successive RR intervals differences), NN50 (the number of interval differences of successive normal to normal RR intervals that are greater than 50 ms ("NN" is used instead of RR to show that the processed beats are considered to be "normal" beats)), and pNN50 (the fraction of NN50 intervals, a proportion of the total number of NN intervals). The frequency-based features refer to the spectral components of HRV (high-frequency power (HF: 0.15–0.4 Hz), low-frequency power (LF: 0.04–0.15 Hz), very-low-frequency power (VLF: 0.003–0.04 Hz), total power, and LF/HF).

Previously, it has been shown that LF and the LF/HF were associated with anxiety [21]; whereas, LF/HF index was related to disgust [22]. Applying some standard features, including spectrum, amplitude, mean, maximum, and SD to the support vector machine (SVM), the highest correct rates of 78.4 and 61.8% were reported for three and four affective states, respectively [23]. Utilizing standard approaches, some other investigations have been done in the study of emotion [7, 24–26].

It has been shown that heart rate regulation is a complex phenomenon, which has nonlinear interactions with some physiological subsystems [27]. As HRV is naturally chaotic, some nonlinear indices have been also employed in the literature. The fractal indices (power-law correlation, detrended fluctuation analysis (DFA), and multifractal analysis), recurrence quantification analysis (RQA), entropy measures (approximate entropy (AE), and sample entropy), Lyapunov exponents (LE), and Poincare plots are some examples of nonlinear features.

In the study performed by Kim and Andre [28], features from different analysis domains, including dynamical characteristics were extracted to classify four emotions in response to music. The recognition accuracy of 70% was reported. Valenza et al. [29] evaluated deterministic chaos, DFA, and RQA parameters in emotion recognition. Using the nonlinear features in combination with the quadratic discriminant classifier, a dramatic increase was observed in emotion recognition rates. The recognition accuracy of >90% was attained [29]. In another study, the team [30] adopted AE and LE as nonlinear characterizations of the HRV during emotion elicitation. A clear distinction between the neutral and the arousal stimuli was reported. To categorize the affective states, different features of HRV including LE were fed into the SVM [15]. An average accuracy of 80% was achieved.

Among the nonlinear approaches, the Poincare based indices play an important role in the biomedical signal processing owing to their simplicity, easy understanding, and interpretation. However, little attention has been paid so far to these measures for emotion recognition compared to other traditional and contemporary features.

Recently, the effects of excitatory and relaxing music on the geometric indices of HRV have been evaluated in healthy women [31] and men [32]. By analyzing Poincare plot measures, a great beat to beat dispersion of RR intervals and a great dispersion of RR intervals over the long-term were reported during heavy metal (excitatory) music. An extremely decrease of global HRV was observed during excitatory music. More recently, Nardelli et al. [10] added some lagged Poincare indices to the various standard based, and nonlinear based features to distinguish four different levels of arousal and two levels of valence. The recognition accuracies of 84.72 and 84.26% were obtained for the valence and arousal dimensions, respectively.

The goal of the current study was to propose an emotion recognition approach based on the HRV measures. The proposed technique comprised of simple, fast, and nonlinear geometrical features derived from the lagged Poincare plots.

This research is organized as follows: First, the process of data acquisition is briefly described. Then, the methodology applied in the current study, which consists of feature extraction and classification, is introduced. Finally, the experimental results are reported and the study is concluded.

Methods

After collecting ECG data (Data collection), signals were preprocessed. AC power line noise (50 Hz) was removed, and the data were segmented according to the emotional loads of the pictures. HRV was estimated from successive RR intervals of ECG signals. Then, some features were extracted from the HRV as indicators of emotional reactions (Feature extraction). Finally, the normalized features [x − mean(x)/std(x), where x is a data point] were applied to the classifier (Classification). Different processing stages have been demonstrated in Fig. 1.

Data collection

Participants

ECG signals of 31 females (age range: 19–25 years; mean age: 21.90 ± 1.7 years) and 16 males (age range: 19–23 years; mean age: 21.1 ± 1.48 years) were recorded while subjects were watching the affective pictures. All the participants were healthy with no history of the neurological, epileptic, cardiovascular, and hypertension diseases. They were asked not to use caffeine, salty or fatty foods 2 h before the experiment. Upon arrival at the laboratory, all the subjects were requested to read and sign a consent form to take part in the study. The privacy rights of human subjects were always observed and the experiment was conducted in accordance with the ethical principles of the Helsinki Declaration [33].

Emotional stimuli

In order to provoke emotions in the subjects, pictures from the international affective picture system (IAPS) were applied [34]. According to the 2D emotion model, the images were grouped into the four emotion classes, including happiness, peacefulness, sadness, and fear (Fig. 2). Each subset was chosen via empirical thresholds on the valence and arousal scores [6].

The whole procedure took about 15 min and images were presented after 2 min of rest. In the preliminary baseline measurement, the participants were taught to keep their eyes open and look at a blank screen. Then, 28 blocks of pictures were randomly demonstrated to prevent habituation in subjects. The blocks were the same among the individuals. five images with a similar affect category were inserted in each block which demonstrated for 15 s. Then, 10 s of the blank screen were included at the end of each block. This process was done to ensure the stability of the emotion over time and to allow the physiological variations return to the baseline. Afterward, a white plus was demonstrated for 3 s on the screen, which prepares the participants for the subsequent block and makes them focus on the center of the screen. Figure 3 demonstrates

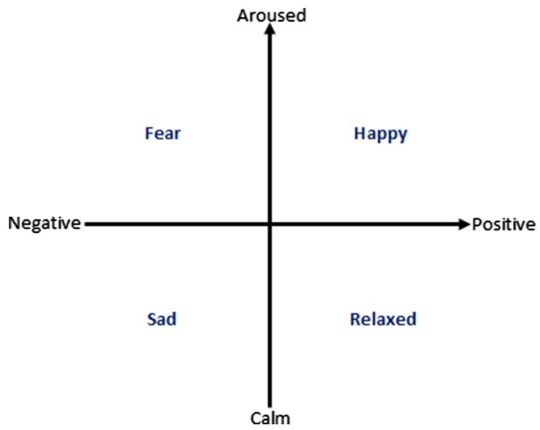

Fig. 2 Dimensional structure of the emotional space

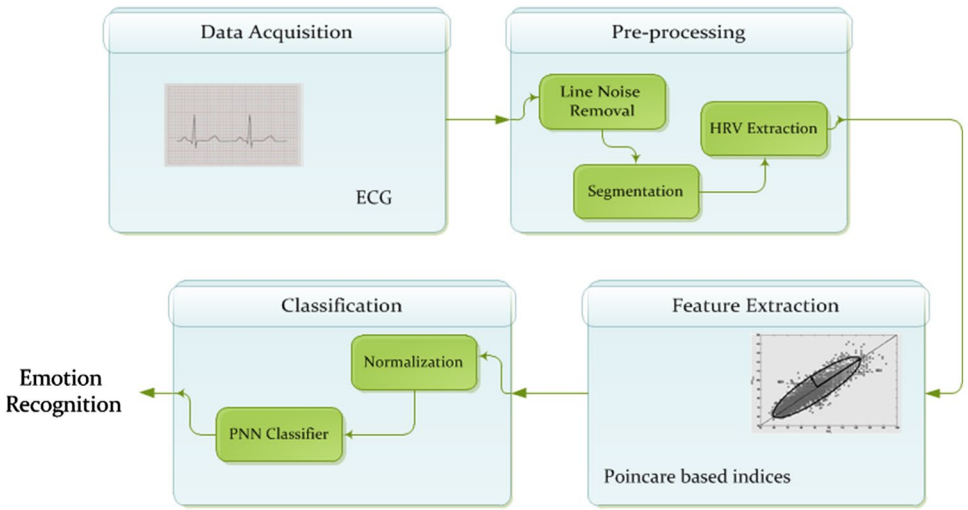

Fig. 1 Proposed methodology applied in current study

Fig. 3 Protocol description

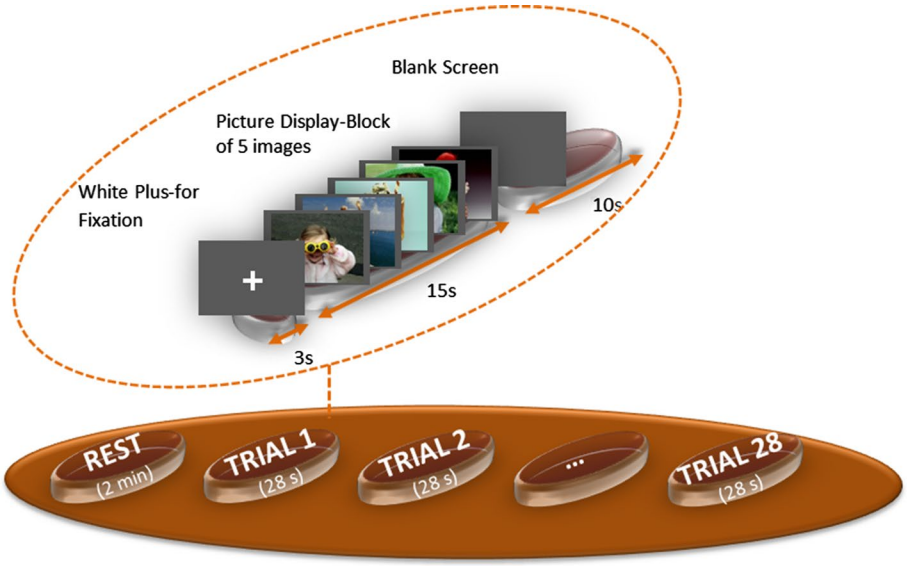

the protocol description. Finally, all the volunteers were requested to describe their emotions through the self-assessment report.

Data recording

A 16-channel PowerLab (manufactured by ADInstruments) with a sampling rate of 400 Hz was used to record ECGs. Taking the advantages of Chart5 for Windows software (ADInstruments), a digital notch filter was adjusted to filter power line noise. Sitting in front of a laptop screen (15.5-inch, VAIO E Series), ECG signals of the subjects were recorded from lead I. The subtle and precise information of the heart, which can be obtained from precordial leads, was not essential for the current study. In addition, limb leads were recorded more easily and the subjects feel more comfortable. Therefore, lead I was chosen. Finally, the ECG beat to beat interval (RR interval) was extracted automatically using Chart5 software (ADInstruments, Australia). Then, the time interval between R-peaks considered as HRV for further processing (based on heart rate = 60/RR interval in seconds).

All signals were collected in Computational Neuroscience Laboratory of the Sahand University of Technology. The laboratory conditions, such as the room light and temperature (23–25 °C), remained unchanged as much as possible.

Feature extraction

Lagged Poincare plot

The Poincare plot is a geometrical representation of a RR time series constructed by plotting successive RR intervals (RR_i, RR_{i+1}) on a 2D phase space. This method has been applied for qualitative visualization, as well as assessing the HRV dynamics [35].

To quantitatively assess the plot, some mathematical descriptors of the shape of the plot have been recommended [30]. By fitting an ellipse to the shape of the Poincare plot, the major and minor axis of the fitted ellipse were considered as two basic descriptors of the plot, namely SD_1 and SD_2. Considering the 45° imaginary diagonal line (Fig. 4), SD_1 and SD_2 represent the dispersion of points perpendicular to and along the line of identity, respectively.

SD_1 describes the short-term variability of HRV, and reflects the parasympathetic activity, while SD_2 refers to the long-term dynamics of HRV, and expresses the overall variability. The SD_1 and SD_2 measures are actually derived from the correlation and mean of the RR

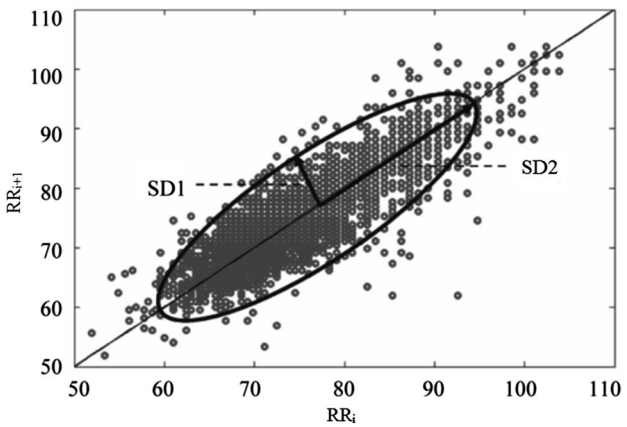

Fig. 4 Graphical representation of the SD1 and SD2 indices

intervals time series with lag-0 and lag-1. By the choice of time delay, the dependency amongst the variables is controlled, and the most common analysis is done with higher order linear correlation between points.

Plotting the 2D phase space with lag-m, the SD_1 and SD_2 can be estimated as follows:

$$SD_1^2 = \gamma_{RR}(0) - \gamma_{RR}(m) \quad \Rightarrow \quad SD_1 = F(\gamma_{RR}(0), \gamma_{RR}(m)) \tag{1}$$

$$SD_2^2 = \gamma_{RR}(0) + \gamma_{RR}(m) - 2\overline{RR}^2 \quad \Rightarrow \quad SD_2 = F(\gamma_{RR}(0), \gamma_{RR}(m)) \tag{2}$$

where $\gamma_{RR}(m)$ is the autocorrelation function for lag-m RR interval and $\overline{RR}$is the average value of RR intervals.

The following Poincare indices were extracted and analyzed from SD_1 and SD_2:

- SD_{12} shows the ratio and balance between short and long variations of RR intervals [36]. In fact, the balance between sympathetic-parasympathetic arms can be represented by SD_{12}. It can be calculated by:

$$SD_{12} = SD_1/SD_2 \tag{3}$$

- S is the area of the ellipse fitted on the Poincare plot [36], which is under the vagal influence.

$$S = \pi \times SD_1 \times SD_2 \tag{4}$$

- SDRR is the variance of the whole HRV series [37] and defined as follows:

$$SDRR = \sqrt{\frac{{SD_1}^2 + {SD_2}^2}{2}} \tag{5}$$

Poincare plots with ten different lags (1–10) were constructed and all indices of the Poincare plot were calculated for each lag. The duration of time series analyzed to obtain Poincare measures was 15 s according to the segments of affective signals.

Classification

The probabilistic neural network (PNN) has been successfully applied to time-series classification [38]. In this network, the distance between the input vector and the training input vectors is computed. By adding some measures, a competitive layer is presented to create the output vector. The second layer gets the maximum probabilities and assigns 1 to that class and 0 to the others. Figure 5 provides a typical architecture.

In terms of structure (Fig. 5), this network consists of Q input/target pairs, which indicates the number of neurons in the first layer, and N elements for each target vector that shows the number of neurons in the second layer. One component of the target vector is 1 and the others are 0. In input, the transpose of the matrix constructed from the Q training pairs considered as the weights of the first layer, $IW_{1,1}$. Upon feeding the input, the closeness of the input vector to the training set vector is calculated which is demonstrated by the ||Dist|| function. Then, the product of the bias in the outputs of ||Dist|| box was sent to transfer function. If an input element is close to a training vector, then the output vector (O_1) adopts a value close to 1.

The target vector (T) was considered as the weights of the second layer, $LW_{1,2}$, in which 1 is allocated to the row related to the certain class of input, and 0's elsewhere. The summation of the elements of O_1 to each of the N input classes resulted in the multiplication TO_1. Finally, the second layer transfer function, which is called the compete layer, dedicated a 1 to the largest element of C box inputs and 0's elsewhere.

The following steps briefly provide an explanation on PNN classification:

1. A feature vector was read by the input layer.

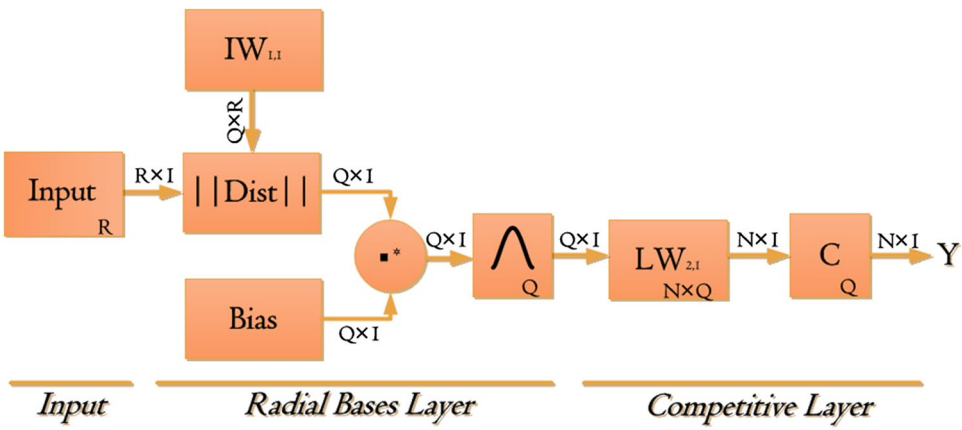

Fig. 5 PNN architecture

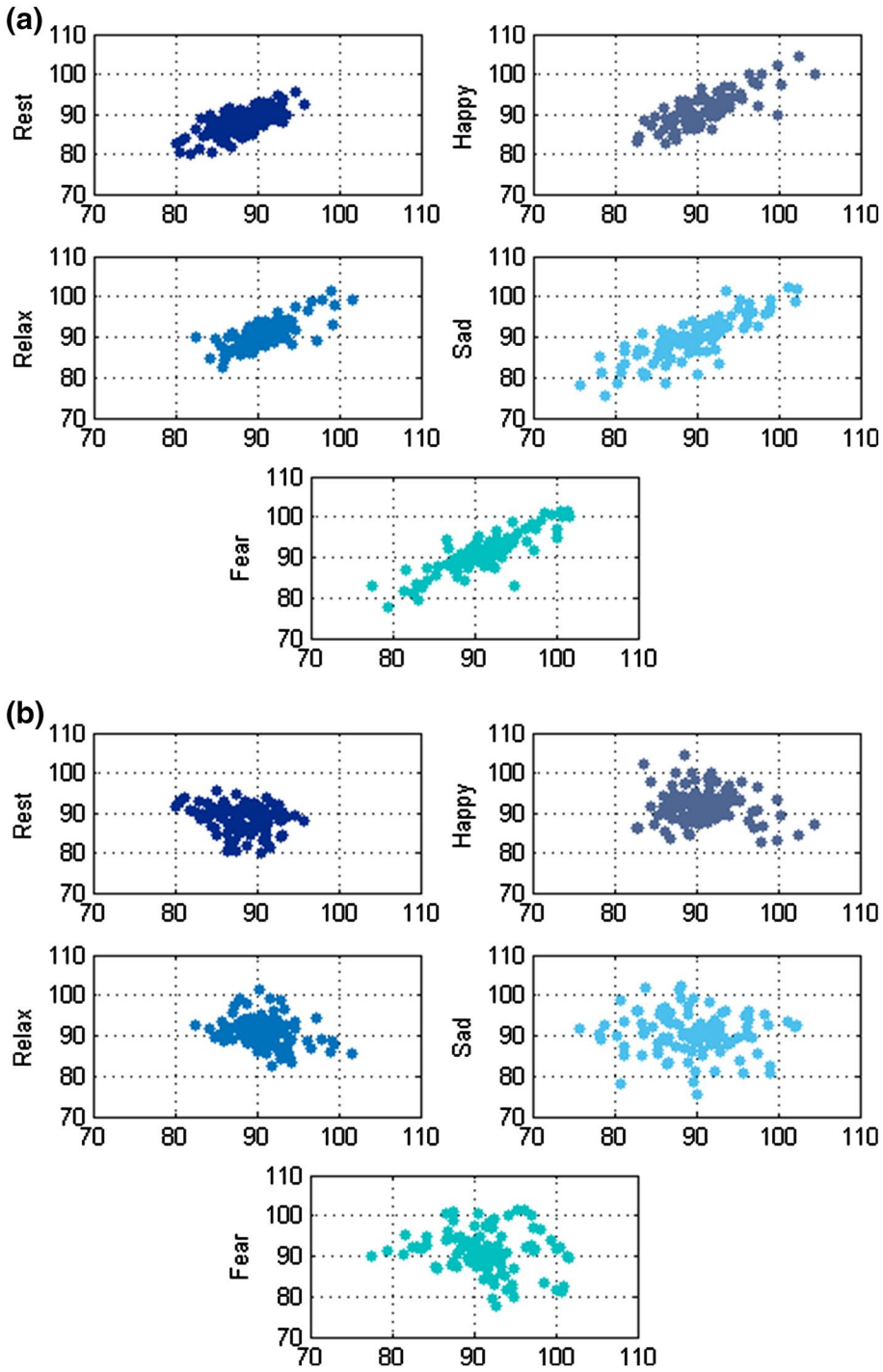

Fig. 6 Poincare plots of different HRV emotional states (record 11) for two lags **a** lag 1 and **b** lag 10

2. The distance between the input and the weight vector is determined, which specifies the closeness of the input to a training set.
3. The summation of these contributions for each input class is determined to produce the probability.
4. A competitive layer selects the maximum of these probabilities and allocates 1 for that class and 0 for the other classes.

In the training process of PNN, the determination of the value of the smoothing parameter–sigma, σ- is an indispensable step. Depending on the data characteristics, the highest classification accuracy is realized for a particular σ. An optimum σ is derived by trial and error. Convergence to a Bayesian classifier is guaranteed by a typical PNN when enough training data are provided. In

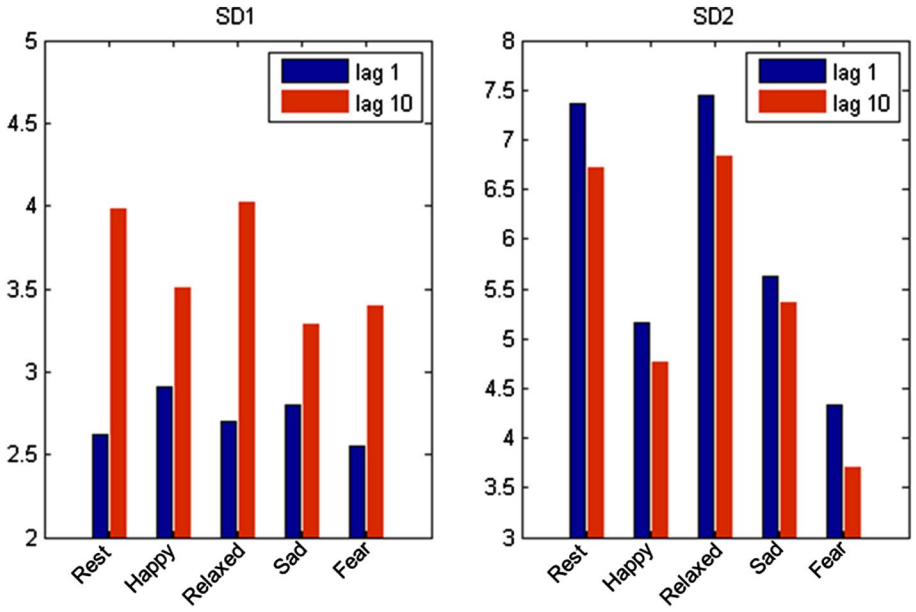

Fig. 7 SD1 and SD2 for two lags (1 and 10) in different emotional states (record 1). The x-axis represents the affective states

addition, the generalization of the PNN is good. In addition, the first layer biases are all set to 0.8326/σ.

Results

Poincare plots with 10 different lags (1 to 10) were constructed. The Poincare plot with lag-1 is shown for rest condition and various emotional states in Fig. 6a. Similarly, Fig. 6b shows the Poincare plots with lag 10 for the equivalent record as in Fig. 6a. As shown in Fig. 6, not only there are morphological differences in Poincare plots between rest condition and affective states, but also as the lag increases the Poincare plots becomes more circular.

The Poincare indices were extracted from each HRV segment in 5 states (the 4 emotion categories and rest condition). To evaluate the effect of emotional stimuli on the Poincare indices with lag 1 and lag 10, Fig. 7 shows the SD_1 and SD_2 values in different affective states in one subject.

As shown in Fig. 7, the SD_1 values in lag 10 were significantly higher than those in lag 1 ($p < 0.05$). Whereas, in higher lags (lag 10) the SD_2 values were lower than those in lag 1.

To carefully evaluate this effect, Fig. 8 shows the influence of the lags on SD_1 and SD_2 within each emotional induction for all subjects.

According to the results, the SD_1 and SD_2 values are affected by different emotional states. In addition, the impact of different lags on SD_1 and SD_2 is not constant. By increasing the lags, the highest increment in SD_1, and the highest decrement in SD_2 are obtained during happiness. The opposite effect is perceived for fear; the lowest increment in SD_1 and the lowest decrement in SD_2 are observed. Therefore, for different lags and for each emotional state, Poincare plots have different shapes. For lag 1, the Poincare plots are more cigar-shaped for relaxing stimuli, whereas round clouds of points are revealed for rest condition. Since other Poincare indices are constructed as a function of SD_1 and SD_2, and their values are directly influenced by the changes in these parameters, they were not reported schematically.

All features were normalized by subtracting the mean input data from each point and divided by its standard deviation. The normalized features were fed into the classifier. Since the experiment consists of 7 blocks for each of the 5 categories, the number of samples for each participant was about 35 points. Therefore, the feature sample size of 1645 was attained for 47 participants. On the other hand, 5 Poincare indices in 10 lags were extracted for each subject. As a result, totally 50 features were extracted. Therefore, the size of feature vector was 1645×50. The classifier randomly chose 2/3 of the feature vector (1097×50) as the training set and the rest of the features considered as the test data (548×50). The classification accuracy was computed as follows:

$$Accuracy = \frac{TP + TN}{TP + FP + FN + TN} \tag{6}$$

where TP: True Positives, TN: True Negatives, FP: False Positives, and FN: False Negatives.

The classification accuracy was examined considering the 4 emotion categories (happiness, sadness, scare, and

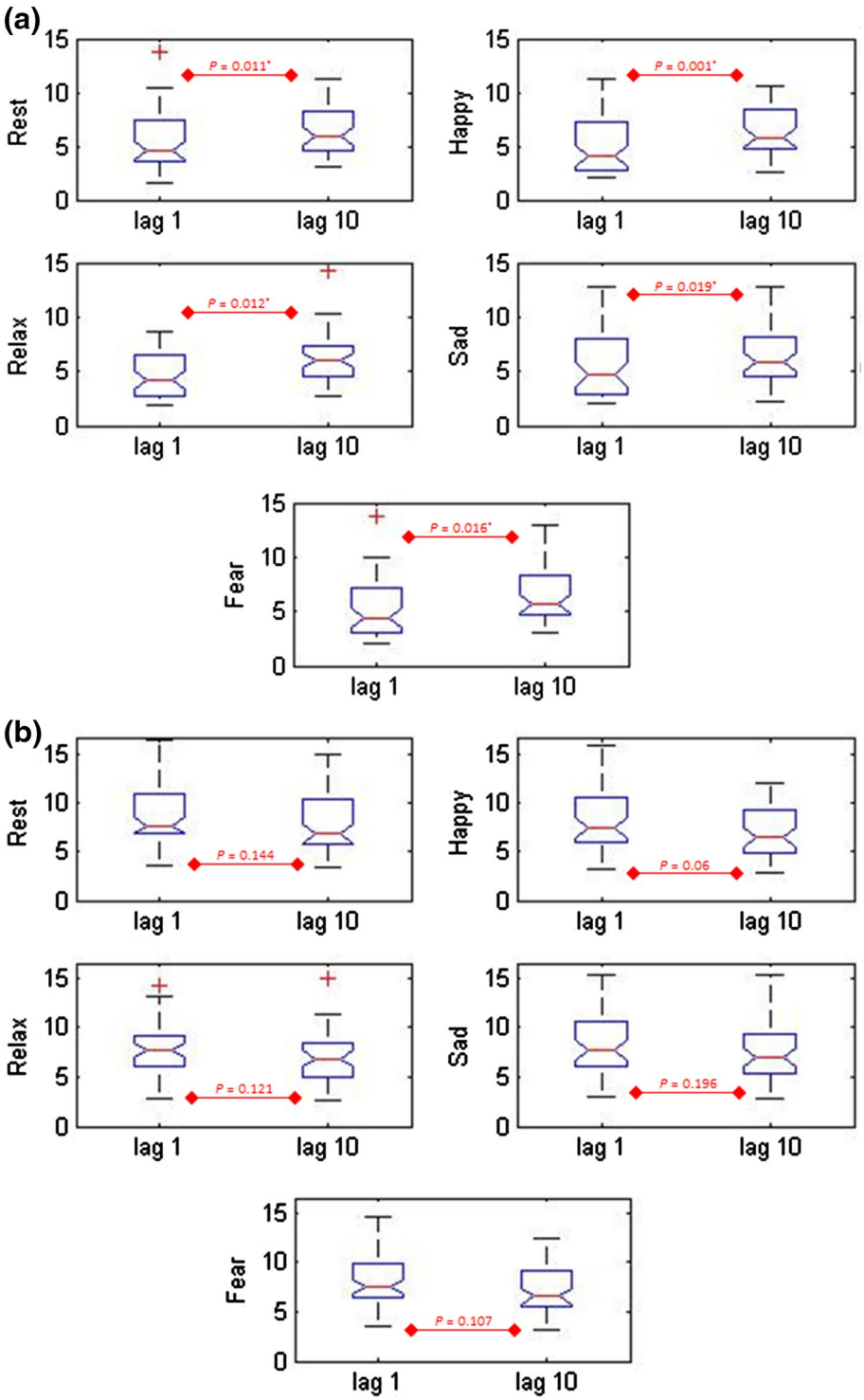

Fig. 8 The influence of two lags of 1 and 10 on HRV Poincare shape in different emotional states for all subjects, **a** SD1, **b** SD2. (*p < 0.05, Wilcoxon rank sum test)

peacefulness) and rest condition as a different class; therefore, 5 classes were defined. The classification results of the proposed methodology are shown in Fig. 9 for different σ.

According to the results, the best classification rate of 97.45% was achieved for σ = 0.03.

Discussion

In the previous decades, several attempts have been performed in order to propose an efficient algorithm for automatic emotion recognition based on physiological signals. The aim of this research was to examine the chaotic nature

of physiological signals for discriminating emotional responses.

The data acquisition protocol and emotion elicitation technique were described in detail. ten lags of Poincare plot were evaluated within five states. For each lag, five geometrical indices were extracted. By increasing the lags, the highest increment in SD_1 and the highest decrement in SD_2 were obtained during happiness, whereas; the lowest increment in SD_1 and the lowest decrement in SD_2 were attained during fearful images. Consequently, it could be concluded that the HRV geometrical shapes and dynamics were significantly changed by the positive- and negative-valence emotions. When relaxing pictures were presented, the Poincare plots were cigar-shaped, which emphasized on the high correlation between RR intervals. In contrast, round clouds of points during rest condition refers to a typical lack of correlation. Significant differences between SD_1 values with lags of one and ten were observed in all affective states (Fig. 8), which confirm the important role of parasympathetic nervous activity in emotion recognition. These results are in agreement with previous findings describing HRV during specific psychophysiological states [10, 39, 40]. To evaluate the ability of features in discriminating emotions, PNN was applied as an automatic classification scheme. The best classification accuracy (97.45%) was attained when σ is 0.03.

Promising results were achieved using simple geometrical indices of HRV. The results of this study are higher than those of previous studies. Zong and Chetouani [41] analyzed ECG, electromyogram, skin conductance, and respiration changes using empirical mode decomposition (EMD) and SVM. The classification rate of 76% was reported. Applying support vector regression to some standard features [42], a maximum accuracy of 90% was provided. Niu et al. [43] employed the genetic algorithm and k-nearest neighbor (KNN) on statistical features of 4 bio-signals. The highest recognition rate of 97% was reported. Applying KNN on the Hurst and higher order spectra parameters of ECG signals [44], the classification accuracy of 93% was achieved. In the study performed by Valenza et al. [15], spectral, higher order spectral representation, and the Lyapunov exponent of HR signals were used as inputs of the SVM. An average accuracy of 80% was achieved. Using EMD and discrete Fourier transform [45], a maximum accuracy of 52% was accomplished with linear discriminant analysis and KNN.

The number of emotions considered in the problem of emotion recognition is an important issue. A maximum classification rate of ~93% has been attained for the classification of six types of emotions from ECG signals [44]. In the present study, five states were classified with the recognition rate of 97.45%.

Previously, it has been proved that autonomic signals such as ECG and HRV have chaotic behavior [46, 47]. In the current study, the reliability of lagged Poincare indices, as an efficient nonlinear approach, in discriminating emotional states was confirmed. The results are in the line with other investigations, which emphasized on the role of nonlinear features in the problem of emotion recognition using autonomic signals [6, 10, 15, 29, 30]. Therefore, the proposed methodology is successful in dealing with the problem of affect recognition.

Conclusion

In conclusion, this study has shown that different affective visual stimuli resulted in different ANS dynamics which can be perceived by the analysis of the geometric parameters of HRV. The experimental results showed that SD_1 can present the dynamic behavior of HRV in different emotional states. Since SD_1 characterizes the dominant action of the parasympathetic activity, the role of the parasympathetic arm is highlighted in visual affective stimuli. In addition, the simplicity, low computational cost, and high accuracy of the proposed algorithm can be served as an automatic online emotion recognition system in the future.

This study has some shortcomings and limitations that should be considered in the future. First, four emotional states were considered in the study. It is suggested that the performance of the proposed methodology with more emotion categories should be evaluated in future studies. Secondly, human emotions are provoked by several induction paradigms like visual, auditory, and tactile modules.

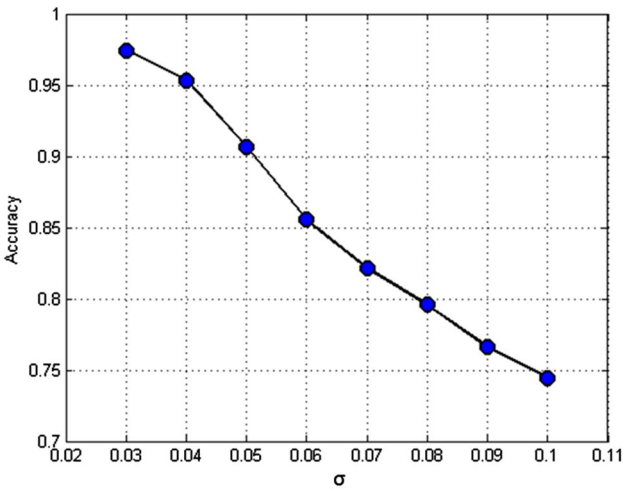

Fig. 9 Emotion recognition rates for different σ values, using proposed methodology

In the current study, the visual paradigm was evaluated by means of static pictures. The future studies should consider the impact of two or more incentive paradigms. Third, the proposed methodology was examined on 47 college students without considering individual characteristics. Therefore, more data with respect to individual differences can be taken into account to strongly confirm the results of the present study. Due to the nature of stimulation, the data were segmented into 15 s windows and the analyses were performed on each segment. However, the window length may influence the HRV results [48]. Therefore, future study should be performed on windows with different lengths and the effect of data length on the proposed methodology should be examined.

Acknowledgements We gratefully acknowledge Computational Neuroscience Laboratory, where the data were collected and all the subjects volunteered for the study.

Compliance with ethical standards

Conflict of interest The authors declare that they have no conflict of interest.

Ethical approval The privacy rights of human subjects were always observed and the experiment was conducted in accordance with the ethical principles of the Helsinki Declaration.

References

1. Ekman P (1999) Basic emotions. In: Dalgleish T, Power M (eds), Handbook of cognition and emotion, Wiley, New York, pp 45–60
2. Smeaton AF, Rothwell S (2009) Biometric responses to music-rich segments in films: the cdvplex. Paper presented at the 7th International Workshop on Content-Based Multimedia Indexing, Chania, Crete
3. Khezri M, Firoozabadi M, Sharafat AR (2015) Reliable emotion recognition system based on dynamic adaptive fusion of forehead biopotentials and physiological signals. Comput Methods Programs Biomed 122(2):149–164
4. Soleymani M, Chanel G, Kierkels J, Pun T (2008) Affective ranking of movie scenes using physiological signals and content analysis. Proceeding of the 2nd ACM workshop on multimedia semantics, New York
5. Verma GK, Tiwary US (2014) Multimodal fusion framework: a multiresolution approach for emotion classification and recognition from physiological signals. NeuroImage 102(1):162–172
6. Goshvarpour A, Abbasi A, Goshvarpour A (2015) Affective visual stimuli: characterization of the picture sequences impacts by means of nonlinear approaches. Basic Clin Neurosci 6(4):209–222
7. Kreibig S, Wilhelm F, Roth W, Gross J (2007) Cardiovascular, electrodermal, and respiratory response patterns to fear and sadness-inducing films. Psychophysiol 44(5):787–806
8. Khalfa S, Roy M, Rainville P, Bella S, Peretz I (2008) Role of tempo entrainment in psychophysiological differentiation of happy and sad music. Int J Psychophysiol 68(1):17–26
9. Goshvarpour A, Abbasi A, Goshvarpour A (2016) Evaluating autonomic parameters: the role of sleep duration in emotional responses to music. Iran J Psychiatry 11(1):59–63
10. Nardelli M, Valenza G, Greco A, Lanata A, Scilingo E (2015) Recognizing emotions induced by affective sounds through heart rate variability. IEEE Trans Affect Comput 6(4):385–394
11. Stemmler G, Heldmann M, Pauls C, Scherer T (2001) Constraints for emotion specificity in fear and anger: the context counts. Psychophysiology 38:275–291
12. Reekum CV, Johnstone T, Banse R, Etter A, Wehrle T, Scherer KR (2004) Psychophysiological responses to appraisal dimensions in a computer game. Cogn Emot 18:663–688
13. Marci C, Glick D, Loh R, Dougherty D (2007) Autonomic and prefrontal cortex responses to autobiographical recall of emotions. Cogn Affect Behav Neurosci 7(3):243–250
14. Vrana S, Rollock D (2002) The role of ethnicity, gender, emotional content and contextual differences in physiological, expressive, and self-reported emotional responses to imagery. Cogn Emot 16:165–192
15. Valenza G, Citi L, Lanata A, Scilingi E, Barbieri R (2014) Revealing real-time emotional responses: a personalized assessment based on heartbeat dynamics. Sci Rep 4:4998
16. Castellano G, Villalba S, Camurri A (2007) Recognising human emotions from body movement and gesture dynamics. Proceedings of the 2nd international conference on affective computing and intelligent interaction, Springer, Berlin
17. Park S, Kim K (2011) Physiological reactivity and facial expression to emotion-inducing films in patients with schizophrenia. Arch Psychiatr Nurs 25(6):e37–e47
18. Schuller B, Arsic D, Wallhoff F, Rigoll G (2006) Emotion recognition in the noise applying large acoustic feature sets proceedings of speech prosody. International symposium on computer architecture, Dresden
19. Sander D, Grandjean D, Scherer K (2005) A systems approach to appraisal mechanisms in emotion. Neural Netw 18(4):317–352
20. Kreibig S (2010) Autonomic nervous system activity in emotion: a review. Biol Psychol 84:394–421
21. Murakami H, Ohira H (2007) Influence of attention manipulation on emotion and autonomic responses. Percept Mot Skills 105:299–308
22. Sokhadze E (2007) Effects of music on the recovery of autonomic and electrocortical activity after stress induced by aversive visual stimuli. Appl Psychophys Biofeedback 32:31–50
23. Kim K, Bang S, Kim S (2004) Emotion recognition system using short-term monitoring of physiological signals. Med Biol Eng Comput 42(3):419–427
24. Demaree H, Schmeichel B, Robinson J, Everhart D (2004) Behavioural, affective, and physiological effects of negative and positive emotional exaggeration. Cogn Emot 18:1079–1097
25. Blechert J, Lajtman M, Michael T, Margraf J, Wilhelm F (2006) Identifying anxiety states using broad sampling and advanced processing of peripheral physiological information. Biomed Sci Instrum 42:136–141
26. Vianna E, Tranel D (2006) Gastric myoelectrical activity as an index of emotional arousal. Int J Psychophysiol 61:70–76
27. Voss A, Schulz S, Schroeder R, Baumert M, Caminal P (2009) Methods derived from nonlinear dynamics for analysing heart rate variability. Philos Trans R Soc Lond A 367(1887): 277–296
28. Kim J, Andre E (2008) Emotion recognition based on physiological changes in music listening. IEEE Trans Pattern Anal Mach Intell 30:2067–2083
29. Valenza G, Lanata A, Scilingo E (2012) The role of nonlinear dynamics in affective valence and arousal recognition. IEEE Trans Affect Comput 3(2):237–249

30. Valenza G, Allegrini P, Lanata A, Scilingo E (2012) Dominant Lyapunov exponent and approximate entropy in heart rate variability during emotional visual elicitation. Front Neuroeng 5:1–7
31. Roque A, Valenti V, Guida H, Campos MF, Knap A, Vanderlei LCM, Ferreira L, Ferreira C, Abreu LD (2013) The effects of auditory stimulation with music on heart rate variability in healthy women. Clinics 68(7):960–967
32. Silva Sd, Guida H, SantosAntonio Ad, Vanderlei LCM, Ferreira LL, de Abreu LC, Sousa F, Valenti V (2014) Auditory stimulation with music influences the geometric indices of heart rate variability in men. Int Arch Med 7(1):1–7
33. World Medical Association (2013) World medical association declaration of Helsinki: ethical principles for medical research involving human subjects. JAMA 310(20):2191–2194
34. Lang P, Bradley M, Cuthbert B (2005) International affective picture system (IAPS): digitized photographs, instruction manual and affective ratings. University of Florida, Gainesville
35. Tulppo M, Makikallio T, Takala T, Seppanen T, Huikuri H (1996) Quantitative beat to beat analysis of heart rate dynamics during exercise. Am J Physiol 271:H244–H252
36. Guzik P, Piskorski J, Krauze T, Schneider R, Wesseling KH, Wykretowicz A, Wysocki H (2007) Correlations between the poincare plot and conventional heart rate variability parameters assessed during paced breathing. J Physiol Sci 57(1):63–71
37. Piskorski J, Guzik P (2005) Filtering poincare plots. Comput Methods Sci Technol 11(1):39–48
38. Belhachat F, Izebodjen N (2009) Application of a probabilistic neural network for classification of cardiac arrhythmias. 13th International research/expert conference on trends in the development of machinery and associated technology (Tmt), Hammamet, Tunisia
39. Goshvarpour A, Goshvarpour A, Rahati S (2011) Analysis of lagged poincare plots in heart rate signals during meditation. Digit Signal Process 21(2):208–214
40. Goshvarpour A, Goshvarpour A (2015) Poincare indices for analyzing meditative heart rate signals. Biomed J 38:229–234
41. Zong C, Chetouani M (2009) Hilbert-Huang transform based physiological signals analysis for emotion recognition. IEEE International Symposium on Signal Processing and Information Technology (ISSPIT), Ajman
42. Chang C-Y, Zheng J-Y, Wang C-J (2010) Based on support vector regression for emotion recognition using physiological signals. The 2010 international joint conference on neural networks (IJCNN). IEEE, Barcelona
43. Niu X, Chen L, Chen Q (2011) Research on genetic algorithm based on emotion recognition using physiological signals. IEEE international conference on computational problem-solving (ICCP), Chengdu
44. Jerritta S, Murugappan M, Wan K, Yaacob S (2013) Classification of emotional states from electrocardiogram signals: a non-linear approach based on hurst. Biomed Eng Online 12:44
45. Jerritta S, Murugappan M, Wan K, Yaacob S (2014) Electrocardiogram-based emotion recognition system using empirical mode decomposition and discrete Fourier transform. Expert Syst 31(2):110–120
46. Wang K, Zhao Y, Sun X, Weng T (2010) A simple way of distinguishing chaotic characteristics in ECG signals. 3rd International conference biomedical engineering and informatics (BMEI), IEEE, pp 713–716
47. Tapobrata L, Upendra K, Hrishikesh M, Subrata S, Arunava Das R (2009) Analysis of ECG signal by chaos principle to help automatic diagnosis of myocardial infarction. J Sci Ind Res 68(10):866–870
48. Dos Santos L, Barroso JJ, Macau ENE, De Godoy MF (2013) Influence of the HRV time series length on the predictive ability for adverse clinical events. Proceeding series of the Brazilian society of applied and computational mathematics, SBMAC, pp 010213-1-010213-5